THE ASTROPHYSICAL JOURNAL, 492:596–602, 1998 January 10

DOES TURBULENT PRESSURE BEHAVE AS A LOGATROPE?

ENRIQUE VÁZQUEZ-SEMADENI, JORGE CANTÓ, AND SUSANA LIZANO
Instituto de Astronomía, Universidad Nacional Autonoma de México, Apdo Postal 70-264, D. F. 04510, México;
enro@astroscu.unam.mx
Received 1997 May 16; accepted 1997 August 22

ABSTRACT

We present numerical simulations of an isothermal turbulent gas undergoing gravitational collapse, with the aim of testing for "logatropic" behavior of the form $P_t \sim \log \rho$, where P_t is the turbulent pressure and ρ is the density. To this end, we monitor the evolution of the turbulent velocity dispersion σ as the density increases during collapse. A logatropic behavior would require $\sigma \propto \rho^{-1/2}$, a result that is not, however, verified in the simulations. Instead, the velocity dispersion *increases* with density, implying a polytropic behavior of P_t. This behavior is found both in purely hydrodynamic and in hydromagnetic runs. For purely hydrodynamic and rapidly collapsing magnetic cases, the velocity dispersion increases roughly as $\sigma \propto \rho^{1/2}$, implying $P_t \sim \rho^2$, where P_t is the turbulent pressure. For slowly collapsing magnetic cases, the behavior is close to $\sigma \propto \rho^{1/4}$, implying $P_t \sim \rho^{3/2}$. We thus suggest that the logatropic "equation of state" may represent only the statistically most probable state of an ensemble of clouds in equilibrium between self-gravity and kinetic support, but does not adequately represent the behavior of the turbulent pressure within a cloud undergoing a dynamic compression as a result of gravitational collapse. Finally, we discuss the importance of the underlying physical model of the clouds (equilibrium versus dynamic) for the results obtained.

Subject headings: ISM: clouds — magnetohydrodynamics — methods: numerical — turbulence

1. INTRODUCTION

Molecular clouds and clumps exhibit the well-known velocity dispersion (or line width) to size relation

$$\sigma \sim R^{1/2} , \tag{1}$$

where σ is the line width–determined velocity dispersion, and R is the characteristic size. This correlation has been observed both in ensembles of clouds (Larson 1981; Leung, Kutner, & Mead 1982; Torrelles et al. 1983; Dame et al. 1986; Myers & Goodman 1988; Falgarone, Puget, & Pérault 1992; Miesch & Bally 1994) and as a function of radius in quiescent cores using various tracers (Fuller & Myers 1992; Caselli & Myers 1995; Goodman et al. 1998), although the latter studies have suggested that the scaling exponent in equation (1) may actually differ between massive and low-mass cores. Furthermore, Goodman et al. (1998) have suggested that the exponent may decrease and approach zero as the innermost regions of the cores, in which the turbulent velocity dispersion becomes subsonic, are considered.

A second scaling relation between mean density $\langle \rho \rangle$ and size, reading

$$\langle \rho \rangle \sim R^{-1} , \tag{2}$$

is also generally reported, although its authenticity has been questioned on theoretical (Kegel 1989; Scalo 1990) and numerical (Vázquez-Semadeni, Ballesteros-Paredes, & Rodríguez 1997) grounds, and significantly discrepant scaling exponents (e.g., Carr 1987; Loren 1989), or none at all (e.g., Plume et al. 1997) have been found. Equations (1) and (2) constitute the now famous Larson's relations.

In spite of the anomalies at small scales and in high-mass regions, Larson's relations are generally accepted as distinctive signatures of turbulence in molecular clouds and clumps (e.g., Larson 1981; Scalo 1987), and together they imply

$$\sigma \propto \rho^{-1/2} . \tag{3}$$

This relation is usually interpreted as a manifestation of virial equilibrium in the turbulent velocity dispersion (possibly magnetohydrodynamic, or MHD) in the clouds (Larson 1981). A turbulent pressure P_t, corresponding to the turbulent velocity dispersion, can then be defined by (Lizano & Shu 1989; hereafter LS)

$$\sigma^2 \equiv (dP_t/d\rho) , \tag{4}$$

in analogy to the relation between thermal pressure and sound speed. Choosing

$$P_t \propto \log \rho \tag{5}$$

recovers the virial relation from equation (3) (LS). Equation (5) is commonly refered to as a "logatropic equation of state,"[1] or simply a "logatrope."

It is important to emphasize that the concept of a turbulent "pressure" may not be a very realistic representation of the effects of turbulence, since it implicitly assumes a microscopic and isotropic process. Turbulence, on the other hand, is a phenomenon involving a wide range of spatial scales, from the scale size of the system under consideration to the smallest dissipative scales. In particular, the existence of large-scale modes implies coherent motions that are more akin to ram pressure (locally anisotropic, with a well-defined direction) than to isotropic, thermodynamic pressure. For these reasons, in the present paper we will focus primarily on the turbulent velocity dispersion. References to turbulent pressure will be made assuming that it can be defined according to equation (4), for compatibility with

[1] Strictly speaking, this is not an equation of state, since it does not involve all three thermodynamic variables. However, we will allow ourselves the terminology for consistency with common nomenclature.

published work, but the above caveat should always be kept in mind.

The logatropic equation of state has been used in a number of studies of cloud support and stability focusing on quasi-static contraction (LS), nonlinear wave propagation (Adams & Fatuzzo 1993; Adams, Fatuzzo, & Watkins 1994; Gehman et al. 1996), and gravitational stability (McLaughlin & Pudritz 1996), among others. Nevertheless, the logatropic equation remains a completely empirical assumption, and there is no direct evidence that turbulent pressure indeed behaves in this manner in fully dynamic situations. In fact, there are some reasons to suggest that it may not:

1. Larson's relations have been observed in either *ensembles* of relaxed clouds (e.g., Torrelles et al. 1983; Dame et al. 1986; Myers & Goodman 1988; Falgarone et al. 1992; Miesch & Bally 1994), or as a function of radius in *quiescent* cores (Fuller & Myers 1992; Caselli & Myers 1995; Goodman et al. 1998), but there is no evidence that they hold in fully dynamical processes, such as gravitational collapse. Interestingly, clouds that are strongly perturbed also seem not to follow the Larson scaling relations (e.g., Loren 1989; Plume et al. 1997). In general, there has been little sampling of fully out-of-equilibrium, dynamical processes, and in particular dynamical collapse has not yet been directly detected because dynamical velocities occur only at very small scales.

2. Although it might be argued that an ensemble of molecular clouds provides a complete sample of various dynamical stages, in actuality most observations are based on clouds and clumps close to *equilibrium*. Thus, the clouds included in surveys such as that of Larson (1989) constitute an ensemble of equilibrium states for clouds of different masses rather than an ensemble of evolutionary steps of a single cloud (of constant mass). That is, instead of representing a number of different states for the same cloud, they represent the same state for different clouds.

3. Vázquez-Semadeni et al. (1997) have suggested that there may exist large numbers of low column density clouds that do not satisfy the density-size relation, and that possibly only the highest column density clouds follow such a scaling relation. Thus, the logatropic equation of state is not expected to apply to such low column density clouds, which are probably not in self-gravitating equilibrium, but rather pressure or ram pressure confined.

As a first attempt to decide this matter, in this paper we present two-dimensional numerical simulations of a turbulent, self-gravitating, magnetized, isothermal gas, with the aim of testing the variation of the velocity dispersion as a cloud is compressed by self-gravity. A related calculation has been performed by Bonazzola et al. (1987), who used low-resolution simulations to estimate the correlation between the nonlinear advection term (related to the turbulent pressure) and the density gradient in a compressible turbulent flow.

We emphasize that the simulations discussed in this paper are not presented as models of cloud cores and their observed line widths, but only as numerical experiments designed to test the applicability of the logatropic equation of state. Furthermore, throughout this paper we will refer exclusively to the *nonthermal* part of the velocity dispersion. In contrast with the observational situation, where the separation between the thermal and nonthermal components is an issue (e.g., Fuller & Myers 1992), in the simulations this is a trivial task, since there is no confusion between the fluid velocity and the thermal velocity dispersion, the latter being directly represented by the temperature field.

The outline of the present paper is as follows. In § 2 we describe the numerical model; in § 3 we present the results for both purely hydrodynamic and fully MHD cases, and in § 4 we summarize and discuss our results.

2. NUMERICAL MODEL

We numerically solve the full MHD equations in two or three dimensions in the presence of self-gravity for an isothermal, gravitationally unstable gas, using the pseudospectral code described in Vázquez-Semadeni, Passot, & Pouquet (1996), although here we restrict ourselves to a scale-free, isothermal case. The equations read

$$\frac{\partial \rho}{\partial t} + \nabla \cdot (\rho \boldsymbol{u}) = \mu \nabla^2 \rho \,, \tag{6}$$

$$\frac{\partial \boldsymbol{u}}{\partial t} + \boldsymbol{u} \cdot \nabla \boldsymbol{u} = -\frac{\nabla P}{\rho} - \left(\frac{J}{M_a}\right)^2 \nabla \phi + \frac{1}{\rho} (\nabla \times \boldsymbol{B}) \times \boldsymbol{B} - \nu_8 \nabla^8 \boldsymbol{u} + \nu_2 \left[\nabla^2 \boldsymbol{u} + \frac{1}{3} \nabla (\nabla \cdot \boldsymbol{u}) \right], \tag{7}$$

$$\frac{\partial \boldsymbol{B}}{\partial t} = \nabla \times (\boldsymbol{u} \times \boldsymbol{B}) - \nu_8 \nabla^8 \boldsymbol{B} + \eta \nabla^2 \boldsymbol{B} \,, \tag{8}$$

$$\nabla^2 \phi = \rho - 1 \,, \tag{9}$$

$$P = c^2 \rho \,, \tag{10}$$

where, as usual, ρ is the density, $\boldsymbol{u}$ is the fluid velocity, P is the thermal pressure, $\boldsymbol{B}$ is the magnetic induction, and ϕ is the gravitational potential. The nondimensionalization is the same as in Passot, Vázquez-Semadeni, & Pouquet (1995), to which we refer the reader for more details of the numerical method. The units are $\rho_0 = \langle \rho \rangle$ (mean density in the integration domain), $u_0 = c_s$ (isothermal speed of sound), L_0 (size of the integration domain $= 2\pi$), $t_0 = L_0/u_0$ (sound crossing time for the integration box), and B_0 (magnetic field strength such that at $\rho = \rho_0$, $v_A = u_0 = c_s$, where v_A is the Alfvén speed). The resulting nondimensional parameters are $J \equiv L_0/L_J$, the number of Jeans lengths in the integration box, and the Mach number of the velocity unit, $M_a = u_0/c_s$. As a result of our choice of units, $M_a \equiv 1$.

Since the method is pseudospectral, it uses periodic boundary conditions and has no numerical dissipation. Owing to the latter condition, dissipative operators need to be included explicitly. We use a combination of ∇^8 "hyperviscosity" and standard second-order viscosity in the momentum and magnetic equations, which allows confinement of dissipative effects to the smallest scales in the simulation, while filtering oscillations in the vicinity of strong shocks (Passot & Pouquet 1988; see also the discussion by Vázquez-Semadeni et al. 1996). We also use a small amount of diffusion in the continuity equation (6), which also helps the code to handle strong shocks. Finally, the Poisson equation (9) is used in a form suitable for handling infinite or periodic media (Alecian & Léorat 1988).

The initial conditions for the simulations have a smooth Gaussian density profile peaked at the center of the integration box, with $\rho_{max} = 3.35\rho_0$ and a FWHM of $0.53L_0$. The

TABLE 1

RUN PARAMETERS

Run	$\rho_{max}/\langle\rho\rangle$[a]	FWHM/L_0[b]	L_J/L_0[c]	u_{rms}/C_s[d]	B_x[e]	μ[f]	ν_2[g]	ν_8[h]
R128	3.35	0.53	0.9	0.8	0	0.03	2.00×10^{-3}	8.12×10^{-12}
R256	3.35	0.53	0.9	0.8	0	0.0075	5.00×10^{-4}	3.13×10^{-14}
R512	3.35	0.53	0.9	0.8	0	0.008	1.25×10^{-4}	2.00×10^{-16}
NT512	3.35	0.53	0.9	0	0	0.008	1.25×10^{-4}	2.00×10^{-16}
M256	3.35	0.53	0.9	0.8	0.2	0.0075	5.00×10^{-4}	3.13×10^{-14}
M512	3.35	0.53	0.9	0.8	0.2	0.008	1.25×10^{-4}	2.00×10^{-16}
MM256.....	3.35	0.53	0.67	0.8	1.0	0.0075	5.00×10^{-4}	3.13×10^{-14}
MM512.....	3.35	0.53	0.67	0.8	1.0	0.008	1.25×10^{-4}	2.00×10^{-16}
3D96	4.93	0.54	0.9	0.8	0	0.013	1.30×10^{-3}	4.00×10^{-9}

[a] Central density of initial density peak in units of mean density.
[b] FWHM of initial density peak in units of box size.
[c] Jeans length in units of box size.
[d] Initial runs turbulent speed in units of sound speed.
[e] Initial strength of uniform magnetic field.
[f] Diffusion coefficient for the continuity equation.
[g] Standard viscosity coefficient.
[h] Hyperviscosity coefficient.

initial velocity field is turbulent, with Gaussian fluctuations of rms amplitude $u_{rms} = 0.8c_s$ and random phases, with exclusively rotational modes (i.e., no compressible motions).

We have performed three nonmagnetic simulations in two dimensions at resolutions of 128, 256, and 512 grid points per dimension, respectively labeled R128, R256, and R512. Except for the resolution and the amount of dissipation (smaller at higher resolution), these runs are identical. A nonturbulent run at a resolution of 512 grid points per dimension, labeled NT512, was also performed in order to test the numerical noise arising from grid discreteness in the calculation of the velocity dispersion (see below). Finally, a three-dimensional run, labeled 3D96, with a resolution of 96 grid points per dimension, was also performed in order to test for dimensional effects.

We also performed four magnetic simulations. For these runs, labeled M256, MM256, M512, and MM512, the initial magnetic field is along the x-direction, with strength $B_x = 0.2$ for the M runs and $B_x = 1.0$ for the MM runs. For all runs except MM256 and MM512, the Jeans length is $L_J = 0.9L_0$, while for MM256 and MM512, $L_J = 0.67L_0$. A summary of the runs and their parameters, including the diffusion coefficients, is given in Table 1. In all cases, $\eta = 0.002$.

The purpose of performing the three nonmagnetic simulations at different resolutions is to test for convergence, in particular with regard to the effect of dissipation. In the magnetic simulations, runs M256 and M512 are respectively similar to R256 and R512 except for the inclusion of the magnetic field. However, the magnetic field strength used in the M runs is quite small, so that the magnetic field does not prevent gravitational collapse. Runs MM256 and MM512 have a larger magnetic field (implying an Alfvén speed equal to the sound speed), somewhat closer to molecular cloud conditions. In order to guarantee that the MM runs still undergo gravitational collapse, a smaller Jeans length was used.

In the simulations, we define the "collapsing cloud" as a circular region within the simulation, centered at the peak of the density distribution (calculated each time) and containing 30% of the total mass. For the turbulent runs this may not be the best approximation, since the cloud shape is not really circular (see Fig. 1). However, using a true Lagrangian cloud boundary would be much more numerically involved, and we feel that our definition still provides reasonably accurate results, since ultimately gravity overpowers the turbulence and the shapes do not differ substantially from circular. For the three-dimensional run, the cloud was defined as the region containing 10% of the total mass.

The computation of the velocity dispersion requires some special care in order to remove the bulk infall velocity. This is a necessary step, since by definition the velocity dispersion is the rms velocity fluctuation, i.e., $\langle(\boldsymbol{u} - \langle\boldsymbol{u}\rangle)^2\rangle$. However, in the present case of a collapsing cloud, the mean velocity is a function of radius.[2] Thus, we use the following procedure. We first compute the average infall speed u_r as a function of radius, and we then compute the velocity dispersion as $\sigma \equiv \langle(\boldsymbol{u}(\boldsymbol{r}) - u_r(r)\hat{\boldsymbol{r}})^2\rangle^{1/2}$, where $\hat{\boldsymbol{r}}$ is the unit vector in the radial direction, and the average is taken over the whole cloud, but using $r = |\boldsymbol{r}|$ at each position. This procedure shows why our Cartesian grid introduces noise: the "circular" paths along which u_r is computed are not a perfect circumference, but rather the best possible approximation on a Cartesian grid, and the grid points on the path are not all at exactly the same distance from the center. Thus, even in the nonturbulent case there will be a systematic velocity dispersion at every radius due to the presence of a radial velocity gradient and to the "thickness" of the circumference, the error being largest at the smallest radii. In order to estimate the magnitude of the numerical noise, we compute the numerical velocity dispersion in the nonturbulent case as well.

3. RESULTS

As a typical example, Figures 1 and 2 show the density and velocity dispersion fields at times $t = 0.9$ and $t = 2.4$, respectively, in nondimensional units for run R512. The former corresponds to the time of minimum velocity disper-

[2] In general, the mean velocity will always be a function of position for a gas mass undergoing a global volume change. The simplest example is a gas mass in a cubic container compressed by a piston on one side. In the direction of compression, the mean flow velocity will be a function of position, being zero at the fixed wall and equal to the velocity of the piston at the side of the piston. If the gas is additionally turbulent, the turbulent motions will be superposed on this mean-flow velocity.

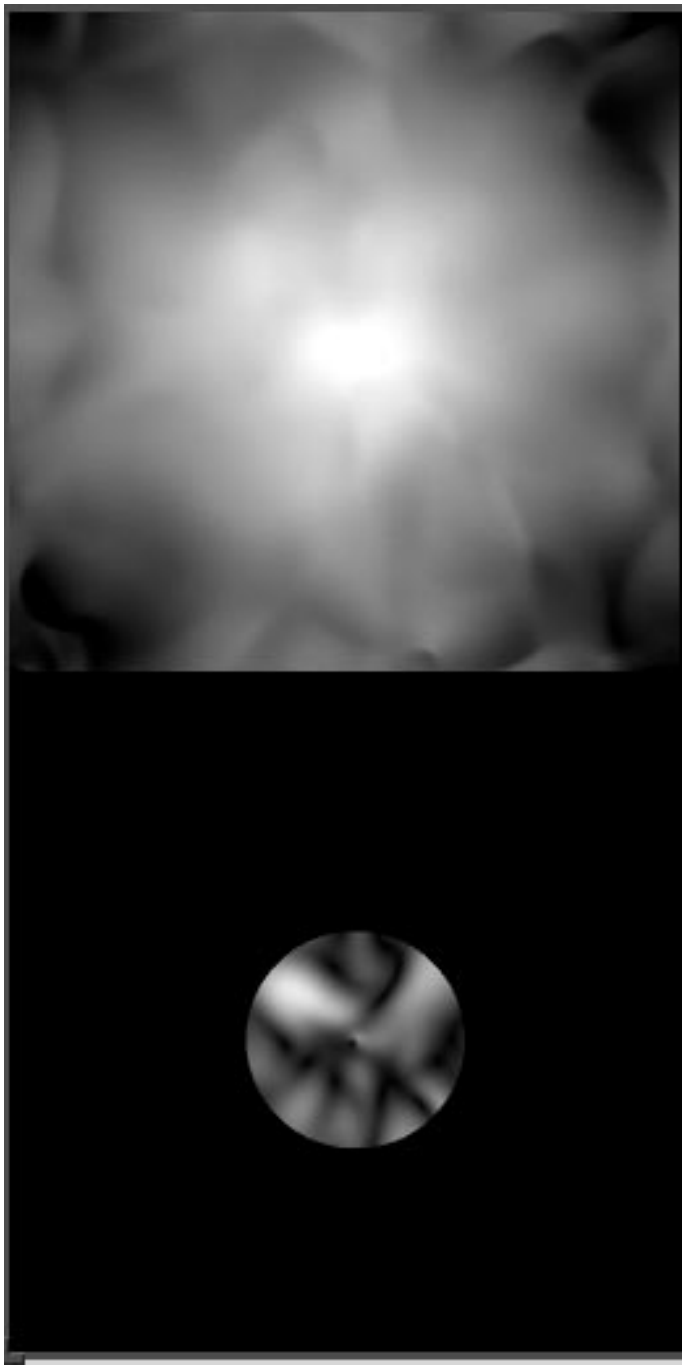

FIG. 1.—Views of the density (*top*) and velocity dispersion (*bottom*) fields for run R512 at time $t = 0.9$ in nondimensional code units. At this time the velocity dispersion is at a minimum, after having been already dissipated by shocks but not yet enhanced by the gravitational compression. The velocity dispersion is shown within a circle containing 0.3 of the total mass in the simulation. The gray scale for the density is logarithmic.

sion, after shocks have dissipated the initial velocity dispersion to a more slowly decaying level, but before compression has begun to enlarge it again (see discussion of Fig. 3 below). The latter time is the final state of the simulation, after which it stops because the code can no longer handle the very large gradients that develop at the center of the cloud.

Figure 3 shows the log of the velocity dispersion plotted against the log of the mean density for all runs as they evolve. For all the turbulent cases, it can be seen that the initial transients suffer significant dissipation through shocks until a less dissipative regime is reached, where the velocity dispersion is a minimum. Subsequently, the velocity dispersion tends to *increase* with mean density, although with significant fluctuations. This behavior is in sharp contrast to equation (3). For the purely hydrodynamic runs R128, R256, and R512, a trend toward longer periods (i.e., larger density ranges) of nearly power-law behavior is noticeable. Although convergence on the duration of the power-law epoch of the evolution may not yet have been reached at 512^2 resolution, the slope does appear to be converging to a value of 1/2. Even if convergence has not

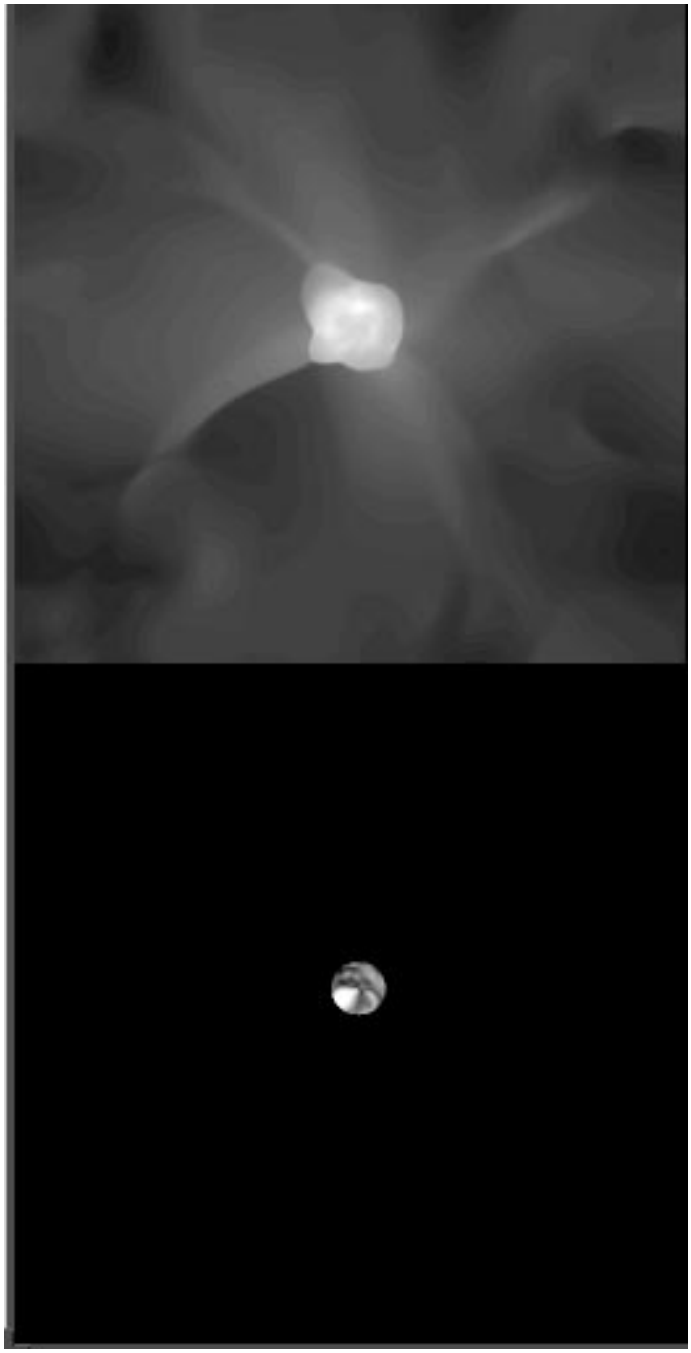

FIG. 2.—Same as Fig. 1, for time $t = 2.4$. This is the final stage of the collapse. Note that the gray scale in this figure differs (has a larger maximum value) from that in Fig. 1 in order to maximize clarity. The maximum density is $\rho_{max} = 330\langle\rho\rangle$.

yet been attained, the observed trend is toward *steeper* slopes at higher resolutions, so in any case the discrepancy with equation (3) appears to be robust.

An important possible problem is that this result might be an effect of the two-dimensionality of the simulations. Run 3D96 was performed as an attempt to resolve this question, although the resolution is necessarily lower. The evolution of the velocity dispersion and the mean density for this run is also shown in Figure 3. Although at much slower rates than in the two-dimensional runs because of the higher dissipation inherent to the lower resolution, the trend in run 3D96 is still toward increasing σ with $\langle\rho\rangle$ after the initial transients have passed. Thus, even though run 3D96 does not permit confirmation of the rates approached by the high-resolution two-dimensional runs, the increasing trend of σ with $\langle\rho\rangle$ is maintained, suggesting that this behavior is real, and not just an effect of the two-dimensionality.

In this regard, note that in general the simulations overestimate the viscous dissipation rate, since for numerical reasons the viscous coefficients must be chosen so that the dissipative scales fit within the resolution of the simulation. In the actual interstellar gas, on the other hand, the dissipation scales may be many orders of magnitude smaller than the scales of interest. Thus, the increase rate of σ found in the simulations is at worst a lower bound to the

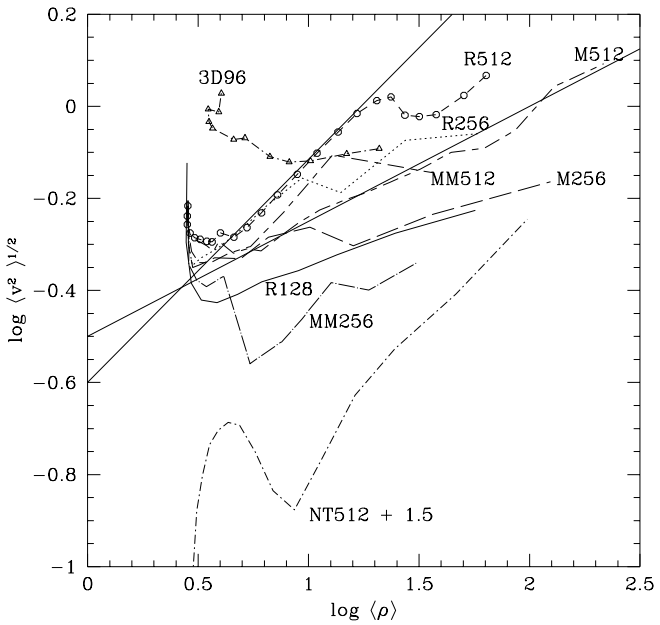

FIG. 3.—The log-log plot of the velocity dispersion vs. average cloud density for all runs. The plot for run NT512 has been displaced upward by 1.5 in the y-axis. In all cases, the velocity dispersion is seen to increase with average density. The circles in the curve for run R512 indicate the individual times during the collapse at which the curve was sampled, taken at intervals $\Delta t = 0.1$ code time units. The two solid straight lines show power laws with exponents 1/2 and 1/4.

actual rate, and the net increase of σ found in the simulations is expected to be a real effect. In particular, run 3D96 is the most dissipative of the runs performed, but a net increase is also found in this case.

The nonturbulent run NT512 also exhibits a velocity dispersion that increases with mean density. This should be interpreted as a numerically generated velocity dispersion that increases at larger infall speeds because the radial velocity gradient is also larger. Nevertheless, this numerical velocity dispersion is seen to be generally about 2 orders of magnitude smaller than that for the turbulent runs (note that the curve for the nonturbulent run has been displaced upward by 1.5 in log σ so that it fits within the plot). Thus, we rule out numerical noise as the cause of the trends observed for the turbulent runs in Figure 3.

The magnetic runs also exhibit a trend of increasing velocity dispersion with increasing mean density, although with quite stronger fluctuations. Runs MM256 and MM512 exhibit a range of densities for which again roughly $\sigma \sim \rho^{1/2}$. Runs M256 and M512 exhibit a somewhat slower dependence, close to $\sigma \sim \rho^{1/4}$. In any case, the general trend is the same as in the nonmagnetic cases, contrary to the logatropic behavior described in equation (3).

4. CONCLUSIONS

4.1. *Summary and Discussion*

We have argued that Larson's (1981) relations and the resulting logatropic "equation of state" (eq. [5]) and virial condition (eq. [3]) may describe an ensemble of clouds *in* (*near*) *equilibrium* between self-gravity and the turbulent velocity dispersion, but not out-of-equilibrium, dynamical processes occurring in a single cloud. We have tested this assertion by means of numerical simulations of collapsing clouds with an initial turbulent velocity field, in both magnetic and nonmagnetic regimes.

The simulations exhibit in all cases a turbulent velocity dispersion that *increases* with mean density as the collapse proceeds, in contradiction to the expected behavior for a logatrope as represented in equation (3). Nonmagnetic and strongly self-gravitating runs seem to approach a power-law behavior of the form $\sigma \sim \langle \rho \rangle^{1/2}$, while weakly self-gravitating magnetic runs in general tend to have shallower dependences, although always with positive exponents. In particular, the fact that magnetic runs exhibit the same qualitative behavior suggests that weak magnetic fields also cannot induce a logatropic (or a $\sigma \sim \rho^{-1/2}$) behavior. Interestingly, run M512 exhibits a behavior very close to $\sigma \sim \rho^{1/4}$. Assuming that this run has converged to the true slope, it is noteworthy that the implied turbulent pressure satisfies $P_t \sim \rho^{3/2}$. This result is consistent with that of McKee & Zweibel (1995) for the polytropic index of Alfvén waves under slow compression. However, runs MM256 and MM512 appear to be closer to the $\sigma \sim \rho^{1/2}$ ($P_t \propto \rho^2$) behavior observed in the nonmagnetic runs. This distinction is likely to be a result of the larger Jeans length used in the M runs, implying a slower collapse (final time $t_{\rm fin} = 2.4$) than for the MM runs ($t_{\rm fin} = 1.0$), so that the M runs are closer to the slow compression assumption of McKee and Zweibel.

We emphasize that although convergence may not yet have been fully achieved at the highest resolution we used (512 × 512 grid points), the trend is toward *faster* increase of the velocity dispersion with density at higher resolution, away from the behavior predicted by the logatropic equation. Thus, the result that velocity dispersion increases with mean density appears quite robust. Moreover, the trend of increasing σ with $\langle \rho \rangle$ is preserved in run 3D96 (albeit at a slower rate owing to the lower resolution of this run), thus ruling out the possibility that our results are a purely two-dimensional effect.

The main consequence of our results is that the logatropic "equation of state" appears to be inadequate for the description of dynamical processes occurring in a cloud. This implies that the use of the logatropic equation in studies of gravitational collapse and dynamical stability is questionable. Its use in studies of quasi-static processes (e.g., LS) may still be justified, although in general the question remains open as to whether the logatropic equation, which can be thought of as representing the *final* states of the virialization process, also represents the behavior of the turbulent pressure *during* the relaxation processes leading to virialization. For this reason, it would also be interesting to test its applicability in problems of nonlinear wave propagation (e.g., Adams & Fatuzzo 1993; Adams, Fatuzzo, & Watkins 1994; Gehman et al. 1996).

Finally, we remark that the ensemble consisting of the evolutionary states of our simulated gravitationally collapsing clouds with fixed mass is completely different from the ensemble constructed from the observations of many clouds of different masses in near equilibrium. The present work shows that for the former ensemble, the logatropic equation of state is not applicable.

4.2. *Comparison with Previous Work*

In our simulations, we obtain a polytropic form $P_t \propto \rho^{\gamma_{\rm eff}}$ for the effective "equation of state" of the turbulence, with polytropic exponents $\gamma_{\rm eff} = 2$ for nonmagnetic and strongly self-gravitating cases, and $\gamma_{\rm eff} = 3/2$ for weakly self-gravitating cases. This result appears to be in contradiction to that of McLaughlin & Pudritz (1996, hereafter MP), who

conclude that the total pressure (thermal plus turbulent) is *not* expected to behave as a polytrope. MP reach this conclusion on the basis of a stability analysis, noting that truncated polytropic solutions with $0 < \gamma_{\rm eff} < 1$ (consistent with the observed lower temperatures of denser structures) never have unstable, or even critically stable, equilibrium solutions. That is, absolutely stable configurations are discarded by MP, so that a cloud is eventually able to collapse and form a star.

It can then be seen that the difference between our results and those of MP arises from a consideration of different physical models of the clouds. While MP's clouds are in hydrostatic equilibrium, our clouds are always out of equilibrium and are already unstable from the start. They may originate from clumps rendered unstable by external turbulent compressions (Vázquez-Semadeni et al. 1996) if the effective equation of state (i.e., the heating and cooling) permits it. In such cases, the clumps need never pass through a static equilibrium state. Another possibility is the well-known onset of gravitational instability arising from the loss of magnetic support caused by ambipolar diffusion (e.g., Nakano 1979; LS).

Finally, we note that the polytropic exponents implied by our simulations are larger than the critical value $\gamma_c = 4/3$ below which gravitational collapse can proceed to a singularity (e.g., Chandrasekhar 1961). Thus, if turbulent pressure continued with this behavior unrestrictedly, it would eventually halt the collapse. However, we do not expect this to occur since, at late stages of the collapse, dissipation becomes important again because of the large velocity gradients that develop. In fact, in Figure 3 an end to the steady increase of σ is seen at large values of $\langle\rho\rangle$ for several of the runs. Thus, we speculate that turbulent pressure cannot by itself halt the collapse.

We would like to acknowledge John Scalo and Steve Shore for useful comments and discussions. This work has made use of NASA's Astrophysical Data System Abstract Service. The runs at 512×512 resolution and run 3D96 were performed on the Cray YPM 4/64 of DGSCA, UNAM. This research has received partial financial support from grants UNAM/DGAPA IN105295, UNAM/CRAY SC007196, and CONACYT 4916-E9406.

REFERENCES

Adams, F. C., & Fatuzzo, M. 1993, ApJ, 403, 142
Adams, F. C., Fatuzzo, M., & Watkins, R. 1994, ApJ, 426, 629
Alecian, G., & Léorat, J. 1988, A&A, 196, 1
Bonazzola, S., Falgarone, E., Heyvaerts, J., Pérault, M., & Puget, J. L. 1987, A&A, 172, 293
Carr, J. S. 1987, ApJ, 323, 170
Caselli, P., & Myers, P. C. 1995, ApJ, 446, 665
Chandrasekhar, S. 1961, Hydrodynamic and Hydromagnetic Stability (Oxford: Clarendon)
Dame, T., Elmegreen, B. G., Cohen, R., & Thaddeus, P. 1986, ApJ, 305, 892
Falgarone, E., Puget, J.-L., & Pérault, M. 1992, A&A, 257, 715
Fuller, G. A., & Myers, P. C. 1992, ApJ, 384, 523
Gehman, C. S., Adams, F. C., Fatuzzo, M., & Watkins, R. 1996, ApJ, 457, 718
Goodman, A. A., Barranco, J. A., Wilner, D. J., & Heyer, M. H. 1998, ApJ, submitted
Kegel, W. H. 1989, A&A, 225, 517
Larson, R. B. 1981, MNRAS, 194, 809
Leung, C., Kutner, M., & Mead, K. 1982, ApJ, 262, 583
Lizano, S., & Shu, F. 1989, ApJ, 342, 834 (LS)
Loren, R. B. 1989, ApJ, 338, 902
McKee, C. F., & Zweibel, E. G. 1995, ApJ, 440, 686
McLaughlin, D. E., & Pudritz, R. E. 1996, ApJ, 469, 194 (MP)
Miesch, M. S., & Bally, J. 1994, ApJ, 429, 645
Myers, P. C., & Goodman, A. A. 1988, ApJ, 329, 392
Nakano, T. 1979, PASJ, 31, 697
Passot, T., & Pouquet, A. 1988, J. Comp. Phys., 75, 300
Passot, T., Vázquez-Semadeni, E., & Pouquet, A. 1995, ApJ, 455, 536
Plume, R., Jaffe, D. T., Evans, N. J., II, Martín Pintado, J., & Gómez-González, J. 1997, ApJ, 476, 730
Scalo, J. M. 1987, in Interstellar Processes, ed. D. J. Hollenbach & H. A. Thronson (Dordrecht: Reidel), 349
———. 1990, in Physical Processes in Fragmentation and Star Formation, ed. R. Capuzzo-Dolcetta, C. Chiosi, & A. di Fazio (Dordrecht: Kluwer), 151
Torrelles, J. M., Rodríguez, L. F., Cantó, J., Carral, P., Marcaide, J., Moran, J. M., & Ho, P. T. P. 1983, ApJ, 274, 214
Vázquez-Semadeni, E., Ballesteros-Paredes, J., & Rodríguez, L. F. 1997, ApJ, 474, 292
Vázquez-Semadeni, E., Passot, T., & Pouquet, A. 1996, ApJ, 473, 881